CrystEngComm

Accepted Manuscript

ROYAL SOCIETY OF CHEMISTRY

www.rsc.org/crystengcomm

Structural directing roles of isomeric phenylenediacetate ligands in the formation of coordination networks based on a flexible *N,N′*-di(3-pyridyl)suberoamide. A rare 5-fold cds net and a 1D network with new mode of entanglement.

Yang-Chih Lo,[a] Wayne Hsu,[a] Hsiu-Yi He,[a]
Stephen T. Hyde,[b]* Davide M. Proserpio[c,d]* and Jhy-Der Chen[a]*

[a]*Department of Chemistry, Chung-Yuan Christian University, Chung-Li, Taiwan, R.O.C.*

[b]*Applied Maths Department, Research School of Physics, Australian National University, Canberra, ACT 0200, Australia*

[c]*Università degli Studi di Milano, Dipartimento di Chimica, Via Golgi 19, 20133 Milano, Italy*

[d]*Samara Center for Theoretical Materials Science (SCTMS), Samara State University, Ac. Pavlov St. 1, Samara 443011, Russia*

Abstract

Reactions of the flexible *N,N′*-di(3-pyridyl)suberoamide (**L**) with Cu(II) salts in the presence of the isomeric phenylenediacetic acids under hydrothermal conditions afforded three new coordination networks, $\{[Cu(\mathbf{L})(1,2\text{-pda})]\cdot H_2O\}_n$ (1,2-H_2pda = 1,2-phenylenediacetic acid), **1**, $\{[Cu(\mathbf{L})(1,3\text{-pda})]\cdot 2H_2O\}_n$ (1,3- H_2pda = 1,3-phenylenediacetic acid), **2**, and $\{[Cu(\mathbf{L})(1,4\text{-pda})]\cdot 2H_2O\}_n$(1,4-$H_2$pda = 1,4-phenylenediacetic acid), **3**, which have been structurally characterized by X-ray crystallography. Complex **1** forms a single 3,5-coordinated 3D net with the $(4^2.6^5.8^3)(4^2.6)$-3,5T1 topology, which can be further simplified as a 6-coordinated $(4^{12}.6^3)$-**pcu** topology. Complex **2** is a 5-fold interpenetrated 3D structure with the $(6^5.8)$-**cds** topology, which exhibits the maximum number of interpenetration presently known for **cds** and complex **3** is the first 1D self-catenated coordination network. The ligand-isomerism of the phenylenediacetate ligands is important in determining the structural types of the Cu(II) coordination networks based on the flexible **L** ligands.

Introduction

The design and synthesis of coordination networks with interesting topologies and potential applications have attracted great attention during recent years.[1] These new complexes thus synthesized are widely applied in catalysis, magnetism materials, gas storage, separation, ion exchange and optical properties. Entanglement is a very interesting phenomenon in coordination networks, and it is also a major factor contributing to the diversities of coordination networks.[2]

The coordination networks of metal complexes containing flexible bidentate ligands are less predictable due to the possible occurrence of supramolecular isomerism involving the adoption of different ligand conformations.[3] However, the flexible ligands with long spacer lengths are prone to form entangled structures due to their inclination to show large voids. Moreover, the dicarboxylate ligands that show diverse coordination ability can be used as auxiliary building blocks in the construction of the coordination networks.[4] Recently, we reported two highly interpenetrated diamondoid nets of Zn(II) and Cd(II) coordination networks, $\{[Zn(\mathbf{L^1})(1,4\text{-BDC})] \cdot H_2O\}_n$ ($\mathbf{L^1}$ = *N,N′*-di(4-pyridyl)adipoamide; 1,4-H_2BDC = 1,4-benzenedicarboxylic acid), and $\{[Cd(\mathbf{L^1})(1,4\text{-BDC})] \cdot 2H_2O\}_n$, which show distorted cages with 8- and 9-fold interpenetrating modes.[3(f)] Combination of a long flexible $\mathbf{L^1}$ ligand with a short rigid 1,4-BDC^{2-} ligands reduced the number of interpenetration as compared with the complex $[CuSO_4(\mathbf{L^1})(H_2O)_2]_n$ featuring a 12-fold interpenetration.[3(c)] We have also shown that increasing the number of the backbone carbon atom of the neutral spacer ligand not only decreases the degree of interpenetration but also changes the structural type.[3(f)]

With this background information, we sought to investigate the influence of geometry and flexibility of the auxiliary dicarboxylate ligand on the structural diversity of coordination networks containing the flexible *N,N′*-di(3-pyridyl)suberoamide (**L**) ligands. The syntheses, structures and properties of $\{[Cu(\mathbf{L})(1,2\text{-pda})]\cdot H_2O\}_n$ [H_2(1,2-pda) = 1,2-phenylenediacetic acid], **1**, $\{[Cu(\mathbf{L})(1,3\text{-pda})]\cdot 2H_2O\}_n$ [H_2(1,3-pda) = 1,3-phenylenediacetic acid], **2**, and $\{[Cu(\mathbf{L})(1,4\text{-pda})]\cdot 2H_2O\}_n$ [H_2(1,4-pda) = 1,4-phenylenediacetic acid], **3**, form the subject of this report.

Experimental

General procedures

IR spectra (KBr disk) were obtained from a JASCO FT/IR-460 plus spectrometer. Elemental analyses were obtained from PE 2400 series II CHNS/O analyzer or a HERAEUS VaruoEL analyzer. Thermal gravimetric analyses (TGA) measurements were carried on a TG/DTA 6200 analyzer of SII Nano Technology Inc. from 30 to 900 °C at a heating rate of 10 ^{o}C min^{-1} under nitrogen. Powder X-ray diffraction instrument were carried on PANalytical PW3040/60 X'Pert Pro diffractometer with a CuK_α (λ_α = 1.54 Å) radiation.

Materials

The reagent $Cu(OAc)_2\cdot H_2O$ was purchased from SHOWA, 1,3-phenylenediacetic acid from Alfa Aesar, and 1,2-phenylenediacetic acid and 1,4-phenylenediacetic acid from ACROS. The ligand *N,N′*-di(3-pyridyl)suberoamide (**L**) was prepared according to a published procedure.[3(d)]

Preparation

{[Cu(L)(1,2-pda)] · H_2O}$_n$, 1.

A mixture of $Cu(CH_3COO)_2 \cdot H_2O$ (0.020 g, 0.10 mmol), L (0.033 g. 0.10 mmol), 1,2-H_2PDA (0.019 g, 0.10 mmol) and 15 mL NaOH (0.04 M) solution was sealed in a 23mL Teflon-lined stainless steel autoclave, which was then heated under autogenous pressure to 120 ^oC for two days. Slow cooling of the reaction system afforded blue crystals suitable for single crystal X-ray diffraction. Yield: 0.026 g (43 %). Anal Calcd for $C_{28}H_{32}N_4CuO_8$ (MW = 616.12, **1** + H_2O): C, 54.58; H, 5.24; N, 9.09 %. Found: C, 55.28; H, 5.48; N, 8.78 %. IR (cm^{-1}): 3442 (m), 2931 (s), 1611 (w), 1545 (w), 1481 (m), 1377 (w), 707 (s).

{[Cu(L)(1,3-pda)] · 2H_2O}$_n$, 2.

Prepared as described for **1**, except that $Cu(BF_4)_2 \cdot H_2O$ (0.023 g, 0.10 mmol) and 1,3-H_2PDA (0.019 g, 0.10 mmol) were used. Yield: 0.025 g (40 %). Anal Calcd for $C_{28}H_{32}CuN_4O_7$ (MW = 600.12, **2** - H_2O): C, 56.04; H, 5.37; N, 9.34 %. Found : C, 55.74; H, 5.20; N, 9.11 %. IR (cm^{-1}): 3267 (s), 1705 (s), 1548 (w), 1483 (s), 1390 (m), 1287 (s), 1158 (s).

{[Cu(L)(1,4-pda)] · 2H_2O}$_n$, 3.

Prepared as described for **1**, except that 1,4-H_2PDA (0.019 g, 0.10 mmol) was used. Yield: 0.020 g (32 %). Anal Calcd for $C_{28}H_{34}N_4CuO_8$ (MW = 618.14): C, 54.40; H, 5.54; N, 9.06 %. Found : C, 54.20; H, 5.07; N, 8.89 %. IR (cm^{-1}): 3289 (m), 3069 (m), 2940 (m), 1712 (s), 1606 (m), 1553 (s), 1478 (m), 1380 (s), 1332 (m), 1294 (m), 1156 (m), 776 (m), 717 (m).

X-ray crystallography

The diffraction data for complexes **1 – 3** were collected on a Bruker AXS SMART APEX II CCD diffractometer at 22 ^oC, which was equipped

with a graphite-monochromated Mo K_α(λ_α = 0.71073 Å) radiation.[5] Data reduction was carried out by standard methods with use of well-established computational procedures.[6] The structure factors were obtained after Lorentz and polarization corrections. An empirical absorption correction based on "multi-scan" was applied to the data for all complexes. The positions of some of the heavier atoms were located by the direct method and the remaining atoms were found in a series of alternating difference Fourier maps and least-square refinements, except that the hydrogen atoms were added by using the HADD command in SHELXTL 5.10. In complexes **1** and **2**, some of the carbon [C(6) – C(9) and C(17) – C(18) for **1** and C(14) for **2**] and oxygen [O(1) and O(17) for **1**] atoms are disordered such that two orientations can be found for each disordered atom. Basic information pertaining to crystal parameters and structure refinement is summarized in Table 1. Selected bond distances and angles are listed in Table 2.

Results and Discussions

Structure of 1

Crystals of **1** conform to triclinic space group $P\bar{1}$ with one Cu(II) cation, two halves of two different **L** ligands and one 1,2-PDA^{2-} anion in the asymmetric unit. Fig. 1(a) shows the coordination environment about the Cu(II) metal center, which is five-coordinated by two pyridyl nitrogen atoms from two **L** ligands and three oxygen atoms from three 1,2-PDA^{2-} ligands, resulting in a distorted square pyramidal geometry with a τ value of 0.32.[7] The Cu(II) ions are linked together by the 1,2-PDA^{2-} ligands that adopt the μ_3-κ^1,κ,$^1\kappa^1$ coordination mode to afford 1D looped chains with dinuclear metal units, Fig. 1(b), which are further connected by the **L** ligands through the pyridyl nitrogen atoms to form a 3D structure. In the structure, the 1,2-PDA^{2-} interact with the **L** ligand through N-H---O

(H---O = 2.02 Å, N---O = 2.86 Å, ∠N-H-O = 162°) hydrogen bonds.

If the Cu(II) cations are defined as 5-coordinated nodes and the 1,2-PDA^{2-} ligands as 3-coordinated nodes, topological analysis reveals that the structure of **1** can be regarded as a 3,5-coordinated net with the $(4^2.6^5.8^3)(4^2.6)$-3,5T1 topology, Fig. 1(c), as determined using TOPOS.[8] If the $Cu_2(\mu\text{-}COO)_2$ dimer is consider as a node, the structure of **1** can be further simplified as a 6-coordinated net with a single $(4^{12}.6^3)$-**pcu** topology, Fig. 1(d). The underlying net 3,5T1 net is observed in 81 crystals (interpenetrated in 13) as can be found in TTD TOPOS database.[9] Interestingly five compounds present dimers $M_2(\mu\text{-}COO)_2$ that allow the same alternative cluster description of the net as **pcu**,[10] with $[Cd(adp)(bpfp)]_n$ [adp = adipate; bpfp = bis(4-pyridylformyl)piperazine] the only one with two different ligands of very different lengths.[10(a)]

Structure of 2

Crystals of **2** conforms to monoclinic space group *C*2/*c* with the Cu(II) cation on the inversion center, with half of **L** and 1,3-PDA^{2-} ligands in the asymmetric unit. The coordination environment about the Cu(II) metal center is shown in Fig. 2(a), which is four-coordinated by two pyridyl nitrogen atoms from two **L** ligands and two oxygen atoms from two 1,3-PDA^{2-} ligands, resulting in a distorted square planar geometry. Two weak Cu---O interactions with the distance of 2.620(4) Å are also observed in the axial positions. The Cu(II) ions are linked together by the 1,3-PDA^{2-} ligands that adopt the μ_2-κ^1,κ,^{1} coordination mode to afford 1D linear chains, Fig. 2(b), which are further linked by the **L** ligands through the pyridyl nitrogen atoms to form a 3D structure.

Each Cu(II) ion is connected to four neighboring Cu(II) ions through

two 1,3-PDA^{2-} and two **L** ligands with distances that are 12.08 Å (through 1,3-PDA^{2-}) and 21.69 (through **L**) and thus each Cu(II) ion can be considered as a four-coordinated node. Topological analysis reveals that complex **2** forms a 5-fold interpenetrated 3D coordination network with the (6^5.8)-**cds** topology, Fig 2(c) and Fig. 2(d). The 5 nets are related by a single translation [0,1,0], so they belong to Class Ia.[11] According to the TTO database of TOPOS,[8,9] the maximum number of interpenetration that has been reported for **cds** in coordination networks is four and there are three examples. Complex **2** thus exhibits the maximum number of interpenetration presently known for **cds**. The five interpenetrated nets are joined in a single net by N-H---O [H---O = 2.06 Å, N---O = 2.90 Å ∠N-H---O = 164^o] hydrogen bonds from the amine hydrogen atoms of the **L** ligands to the carboxylate oxygen atoms of the 1,3-PDA^{2-} ligands, Fig. S4. The water molecules are also involved in hydrogen bonds with the 1,3-PDA^{2-} ligands through O-H---O (H---O= 1.91 and 2.25 Å, O---O = 2.76 and 3.02 Å, ∠O-H---O = 179 and 151^o.

Structure of 3

Crystals of **3** conforms to the orthorhombic space group *Pmna* with the Cu(II) cation lying on a mirror plane, with half of **L** and 1,4-PDA^{2-} ligand and two cocrystallized water molecules in the asymmetric unit. Fig. 3(a) shows the coordination environment about the Cu(II) metal center, which is five-coordinated by two pyridyl nitrogen atoms from two **L** ligands and three oxygen atoms from three 1,4-PDA^{2-} ligands, resulting in a distorted square pyramidal geometry with a τ value of 0.06. The Cu(II) ions are bridged by the 1,4-PDA^{2-} anions that adopt the μ_3-κ^1,κ^1,κ^1 coordination mode to form dinuclear units with a Cu---Cu distance of 3.309(1) Å, which are further linked by the **L** ligands and the 1,4-PDA^{2-} ligands to form a 1D self-catenated coordination network, Fig. 3(b) and

Fig. 3(c). It can be seen that each of the 34-membered rings that involves two Cu(II) ions and two **L** ligands is penetrated by two 1,4-PDA^{2-} ligands. Adjacent 1D chains are connected by water molecules through N-H---O (H---O = 2.14 Å, N---O = 3.00 Å, ∠N-H---O = 177°) hydrogen bonds originating from the amine hydrogen atoms of the **L** ligands to the water molecules, and O-H---O (H---O = 1.82 – 1.93 Å, O---O = 2.65 – 2.76 Å ∠O-H---O = 164 - 168°) hydrogen atoms to the carboxylate oxygen atoms of 1,3-PDA^{2-} ligands, Fig. S5.

Self-catenated nets are single nets that exhibit the peculiar feature of containing shortest rings through which pass other components of the same network.[12] Catenation can be identified by the presence of edge(s) that thread a ring, in other words, they share at least one point with a disc-like film bounded by the ring. Since infinite nets with three lattice vectors inevitably contain large cycles that are threaded, we restrict "rings" to smallest cycles in the net, that cannot be decomposed into sums of still smaller cycle, such as "strong rings.[13] If both the threaded edge and the ring belong to a single connected component of the structure, it is self-catenated. Most coordination networks showing the feature of self-catenation are 3D nets,[14] and there are only several 2D cases that are presently known.[15] Complex **3** thus appears to be the first 1D coordination network showing self-catenation.

This network has an additional feature that is worth noting, namely, it is entangled. To see this, it is convenient to redraw complex **3** as a "ladder" (with single back- "/" and paired forward-slash"\" stringers), shown in Fig. 4(a). Here the structure has been redrawn to preserve its topology. Further, though its geometric details (such as vertex locations and bonding geometries) are distorted, its tangled features, namely the

mutual catenation of edges and cycles, are also preserved. This means that the structure of Fig. 4(a) is an equivalent "tangled-isotope" that preserves both the topology and the edge crossings . Here we adopt the term "tangled-isotope" from the mathematical operation of "ambient isotopy", corresponding to distortions of a structure that do not alter its inherent entanglement.[16] The ring formed by a pair of forward-slashes -- one above and one below -- sharing two vertices is threaded by (two parallel) back-slashes, describing the self-catenations. A simpler, untangled-isotope is that whose pair of forward-slash stringers are either both above or both below the back-slash stringers, illustrated in Fig. 4 (b). The edges of this untangled-isotope reticulate a cylinder without any edge crossings (with forward- and back-slashes running on opposite faces of the cylinder). In contrast, the edges of complex **3** cannot reticulate a cylinder without edge crossings: a multi-handled surface made of a pair of parallel cylinders with connecting tubes is necessary to support a crossing-free reticulation. Since this latter surface is topologically more complex than the simple cylinder, complex **3** is (according to the definition advanced in reference 15) entangled.

Closely related tangled-isotopes to complex **3** are knotted, with more common signatures of entangled networks in terms of the constituent knots or links. For example, permutations of the crossings between forward- and back-slash stringers result in patterns containing threaded links, or pairs of catenated rings. Two of the simpler tangled-isotopes are those with Hopf links, Fig 4(c), and Solomon links, Fig. 4(d). In start contrast to complex **3**, both of these are tangled-isotopes, since they contain pairs of interwoven cycles that cannot be separated without breaking edges, illustrated in the Figures. They are distinguished by the crossings of one cycle (blue in the Figures) with the interlocked (black)

cycle. If we denote crossings of blue edges over / under black edges by the symbols "+" / "-", an anti-clockwise walk around a blue cycle made of four edges in Figure 4(c) crosses black edges in the order "- + + +" (or cyclic permutations); the analogous walk in Fig. 4(d) is "+ - + -". These sequences of over and under crossings characterise Hopf and Solomon links respectively (see, for example, reference 17). However, the entanglement in complex **3** is a peculiar and hitherto unrecognised one. It has neither knots nor links. Further, it is also free of "ravels" -- a subtle entanglement mode distinct from knots or links -- that can be formed in tangled nets.[18] To date, knots, links and ravels have all been identified in metal-organic complexes.[2,19] Complex **3** is, to our knowledge, the first example of a tangled net that contains neither knots, links nor ravels, thus exemplifying a new mode of entanglement.

Ligand conformations and structural comparisons

Twenty ligand conformations can be found for **L** if the A and G conformations are given when the C-C-C-C torsion angle (θ) is $0 \leq \theta \leq 90^{o}$ and $90 \leq \theta < 180^{o}$, respectively. In addition, based on relative orientation of the C=O groups, each conformation can adopts *cis* or *trans* arrangement. Moreover, due to the difference in the orientations of the pyridyl nitrogen atom positions, three more orientations, *anti-anti*, *syn-anti* and *syn-syn*, based on the relative positions of the pyridyl nitrogen and amide oxygen atom can also be derived, Fig. 5.

Table 3 lists all the ligand conformations of the **L** ligands in complexes **1** – **3**. The structural parameters of the reported complexes $[Cu(\mathbf{L})(1,2\text{-bdc})]_n$ (1,2-H_2bdc = 1,2-benzenedicarboxylic acid) and $[Cu(\mathbf{L})(1,3\text{-bdc})(H_2O)\cdot 3H_2O]_n$ (1,3-H_2bdc = 1,3-benzenedicarboxylic

acid) that contain **L** are also shown for comparison.[20] A comparison of these structures shows that the flexibility of the dicarboxylate ligands, in which the pda^{2-} ligands in **1** – **3** hold two more CH_2 groups than the bdc^{2-} ligands, significantly affects the structural diversity. In **1** and $[Cu(1,2\text{-bdc})(\mathbf{L})]_n$, the 1,2-$pda^{2-}$ and 1,2-bdc^{2-} ligands adopt the μ^3-κ^1,κ^1,κ^1 mode and μ^2-κ^2,κ^2 mode, respectively, resulting in AAAAA *trans anti-anti* and GGAGG *trans anti-anti* conformations for the **L** ligands in **1** and AAAAA *trans syn-syn* conformation for the **L** ligands in $[Cu(1,2\text{-bdc})(\mathbf{L})]_n$, forming a 3D structure with 3,5T1 topology and a 2D wavelike structure, respectively. In contrast, the 1,3-pda^{2-} and 1,3-bdc^{2-} ligands of **2** and $[Cu(1,3\text{-bdc})(\mathbf{L})(H_2O)] \cdot 3H_2O$ adopt the same μ^2-κ^1,κ^1 coordination mode, but lead to the formation of AAAAA *trans anti-anti* conformation for the **L** ligands in **2** and GAAAG *trans syn-syn* and AAAAA *trans syn-syn* conformations for the **L** ligands in $[Cu(1,3\text{-bdc})(\mathbf{L})(H_2O)] \cdot 3H_2O$, resulting in 5- and 3-fold interpenetration, respectively. In each single **cds** structure, the distances between the Cu(II) nodes are 12.08 Å (through 1,3-pda^{2-}) and 21.69 Å (through **L**) for **2** significantly longer than those of 9.66 Å (through 1,3-bdc^{2-}) and 19.46 Å (through **L**) for $[Cu(1,3\text{-bdc})(\mathbf{L})(H_2O)] \cdot 3H_2O$, indicating the importance of the length of the spacer ligand in determining the number of interpenetration. The *cis*- and *trans*-conformations of the phenylenediacetate ligands have been investigated recently.[21] For example, in the 1D ladder-like silver(I) complex $[Ag_3(cis\text{-pda})(bipy)_3]_n \cdot 0.5n(trans\text{-pda}) \cdot 5nH_2O$ (bipy = 4,4'-bipyridine), both of the two different formations (*cis*- and *trans*) of the 1,2-pda^{2-} ligands were observed.[21a] Inspection of the structures of the three isomeric pda^{2-} ligands in **1** - **3** reveals that they all adopt the *trans*-conformations.

Thermal properties

In order to estimate the stability of the frameworks, thermogravimetric analysis (TGA) of complex **1 - 3** was carried out in nitrogen atmosphere from 30 to 900 ^{o}C, Fig. S6 and Table S1. The TGA curve of **1** shows the gradual weight loss of water molecules (calculated 5.02 %; observed 3.53 %) in 50 - 190 ^{o}C. The weight loss between 200 - 460 ^{o}C corresponds to the decomposition of **L** ligand and 1,4-pda^{2-} ligand (calculated 84.96 %; observed 86.41 %). The TGA curve of **2** shows the gradual weight loss of water molecules (calculated 3.00 %; observed 2.16 %) in 45 - 200 ^{o}C and the weight loss of 86.19 % between 200 - 510 ^{o}C corresponds to the decomposition of **L** ligand and 1,4-pda^{2-} ligand (calculated 86.41 %). For complex **3**, the TGA curve shows the gradual weight loss of water molecule (calculated 5.83 %, observed 6.56 %) in 50 - 200 ^{o}C. The weight loss of 83.26 % between 200 - 460 ^{o}C can be ascribed to the decomposition of **L** ligand and 1,4-pda^{2-} ligand (calculated 83.89 %). The TGA results show that the weight losses that are due to the removal of cocrystallized and the bonded water molecules occurred in 45 – 200 ^{o}C, and the organic ligands decomposed at temperatures above 200 ^{o}C. The different structural types of **1** – **3** do not affect the decomposition of the organic ligands significantly. The PXRD patterns of complexes **1** – **3** heated at 150 ^{o}C for 3 hours, Fig. S1 – Fig. S3, reveal that their structures are stable upon the solvent removal. It is noted that the solvent-accessible volumes of complexes **1 - 3** calculated by PLATON[22] after the removal of the water molecules are small as 67.5, 161.0 and 196.2 Å^3, which are 5.0, 5.7 and 6.9 % of each of the unit cell volume, respectively.

Conclusion

Three new coordination networks containing **L** and isomeric

phenylenediacetate ligands have been successfully synthesized under hydrothermal condition. The different structures in **1** - **3** can be attributed to the ligand isomerism of the PDA^{2-} ligands that result in different **L** conformations. Obviously, the **L** ligands are sufficiently flexible to adjust to the stereochemical requirements for the formation of the complexes **1** - **3**, which adopt the conformations that maximize their intra- and intermolecular forces. To our best knowledge, complex **1** is a rare example with two different ligands of very different lengths, with underlying nets 3,5T1 further simplified to **pcu**, complex **2** shows the maximum number of interpenetration presently known for **cds** coordination networks and complex **3** is the first 1D self-catenated, entangled, unknotted and unravelled coordination network.

Electronic supplementary information (ESI) available: PXRD patterns for **1** – **3** (Fig. S1 – Fig. S3). Drawings showing the hydrogen bonds in **2** and **3** (Fig. S4 – Fig. S5). TGA curves for **1** – **3** (Fig. S6). Thermal properties of **1** – **3** (Table S1). CCDC no. 1014134 - 1014136. For ESI and crystallographic data in CIF or other electronic format see DOI: xxxx.

Acknowledgments

We are grateful to the Ministry of Science and Technology of the Republic of China for support. DMP acknowledges the Ministry of Education and Science of Russia (Grant 14.B25.31.0005).

References

1 (a) E. R. T. Tiekink and J. J. Vittal, *Frontiers in Crystal Engineering*, John Wiley & Sons, Ltd., England, 2006; (b) C. B. Aakeröy, N. R. Champness and C. Janiak, *CrystEngComm*, 2010, **12**, 22; (c) M.

O'Keeffe, M. A. Peskov, S. J. Ramsden and O. M. Yaghi, *Acc. Chem. Res.*, 2008, **41**, 1782; (d) J. R. Li, R. J. Kuppler and H. C. Zhou, *Chem. Soc. Rev.*, 2009, **38**, 1477; (e) M. D. Allendorf, C. A. Bauer, R. K. Bhakta and R. J. T. Houk, *Chem. Soc. Rev.*, 2009, **38**, 1330; (f) B. Moulton and M. J. Zaworotko, *Chem. Rev.*, 2001, **101**, 1629; (g) W. L. Leong and J. J. Vittal, *Chem. Rev.*, 2011, **111**, 688; (h) Z. Niu and H. W. Gibson, *Chem. Rev.*, 2009, **109**, 6014.

2. (a) L. Carlucci, G. Ciani and D. M. Proserpio, *Coord. Chem. Rev.*, 2003, **246**, 247; (b) D. M. Proserpio *Nat. Chem.*, 2010, **2**, 435; (c) L. Carlucci, G. Ciani, D. M. Proserpio, T.G. Mitina and V.A. Blatov, *Chem. Rev.*, 2014, **114**, 7557; (d) G.-P. Yang, L. Hou, X.-J. Luan, B. Wu and Y.-Y. Wang, *Chem. Soc. Rev.*, 2012*,* **41***,* 6992; (e) J.-Q. Liu, Y.-Y. Wang, P. Liu, Z. Dong, Q.-Z. Shia and S. R. Batten, *CrystEngComm*, 2009, **11**, 1207.
3. See, for examples: (a) L. Carlucci, G. Ciani, D. M. Proserpio and S. Rizzato, *CrystEngComm*, 2002, **4**, 121; (b) H.-C. Chen, H.-L. Hu, Z.-K. Chan, C.-W. Yeh, H.-W. Jia, C.-P. Wu, J.-D. Chen, and J.-C. Wang, *Cryst. Growth Des.*, 2007, **7**, 698; (c) Y.-F. Hsu, C.-H. Lin, J.-D. Chen and J.-C. Wang, *Cryst. Growth Des.*, 2008, **8**, 1094; (d) Y.-F. Hsu, H.-L. Hu, C.-J. Wu, C.-W. Yeh, D. M. Proserpio and J.-D. Chen, *CrystEngComm*, 2009, **11**, 168; (e) Y.-F. Hsu, W. Hsu, C.-J, Wu, P.-C. Cheng, C.-W. Yeh, W.-J. Chang, J.-D. Chen and J.-C. Wang, *CrystEngComm*, 2010, **12**, 702; (f) J.-J. Cheng, Y.-T. Chang, C.-J. Wu, Y.-F. Hsu, C.-H. Lin, D. M. Proserpio and J.-D. Chen, *CrystEngComm.*, 2012, **14**, 537.
4. (a) M. Du, X.-J. Jiang and X.-J. Zhao, *Chem. Commun.,* 2005, 5521; (b) M. Du, Z.-H. Zhang, X.-G., Wang, L.-F. Tang and X.-J. Zhao, *CrystEngComm*, 2008, **10**, 1855; (c) M. Du, X.-J. Jiang and X.-J. Zhao, *Inorg. Chem.*, 2007, **46**, 3984; (d) J. Yang, J.-F. Ma, Y.-Y. Liu, J.-C.

Ma and S.R. Batten, *Cryst. Growth Des.*, 2009, **9**, 1894.

5 Bruker AXS, APEX2, V2008.6; SADABS V2008/1; SAINT V7.60A; SHELXTL V6.14; Bruker AXS Inc., Madison, Wisconsin, USA, 2008.

6 G. M. Sheldrick, *Acta Crystallogr.*, 2008, **A64**, 112.

7 A. W. Addison, T. N. Rao, J. Reedijik, J. V. Rijn and G. C.Verschoor, *J. Chem. Soc. Dalton Trans.*, 1984, 1349.

8 V. A. Blatov, A. P. Shevchenko, D. M. Proserpio, *Cryst. Growth Des.* 2014, **14**, 3576. See also: http://www.topos.samsu.ru/.

9 E. V. Alexandrov, V. A. Blatov, A. V. Kochetkov and D. M. Proserpio *CrystEngComm*, 2011, **13**, 3947.

10 (a) PECJIS: A. L. Pochodylo and R. L. LaDuca, *Inorg. Chim. Acta*, 2012, **389**, 191; (b) SUNHEP, SUNHIT, SUNHOZ : J. Zhang, T. Wu, S. Chen, P. Feng and X. Bu, *Angew. Chem., Int. Ed.*, 2009, **48**, 3486; (c) QUJHIN: F. Guo, *J. Coord. Chem.*, 2009, **62**, 3621.

11 V. A. Blatov, L. Carlucci, G. Ciani and D. M. Proserpio, *CrystEngComm*, 2004, **6**, 377

12 L. Carlucci, G. Ciani, D.M. Proserpio in *Making crystals by design: methods, techniques and applications*, ed. D. Braga, F. Grepioni Wiley-VCH, Weinheim, 2007, Ch. 1.3, 58.

13 O. Delgado-Friedrichs and M. O'Keeffe, *J. Solid State Chem.,* 2005, **178**, 2480.

14 Xi-Jun Ke , Dong-Sheng Li and Miao Du, *Inorg. Chem. Commun.*, 2001, **14**, 788.

15 See for examples: (a) M. J. Plater, M. R. S. J. Foreman, T. Gelbrich and M. B. Hursthouse, *J. Chem. Soc., Dalton Trans*., 2000, 1995; (b) L.-P. Zhang, J. Yang, J.-F. Ma, Z.-F. Jia, Y.-P. Xie and G.-H Wei, *CrystEngComm*, 2008, **10**, 1410; (c) Y.-Y. Liu, Z.-H. Wang, J. Yang, B. Liu, Y.-Y. Liu and J.-F. Ma, *CrystEngComm*, 2011, **13**, 3811; (d) Y.-Y. Liu, H.-Y. Liu, J.-F. Ma, Y. Yang and J. Yang, *CrystEngComm*, 2013,

15, 1897; (e) Y. Gong, P. G. Jiang, J. Li, T. Wu, and J. H. Lin, *Cryst. Growth Des*., 2013, **13** ,1059; (f) D.-R. Xiao, Y.-G. Li, E.-B. Wang, L.-L. Fan, H.-Y. An, Z.-M Su, and L. Xu, *Inorg. Chem*. 2007, **46**, 4158; (g) R. Custelcean and M. G. Gorbunova, *CrystEngComm*, 2005, **7**, 297; (h) K. Zhou, F.-L. Jiang, L. Chen, M.-Y. Wu, S.-Q. Zhang, J. Ma and M.-C. Hong, *Chem. Commun*., 2012, 5521; (i) G. O. Lloyd, J. L. Atwood, L. J. Barbour, *Chem. Commun.*, 2005, 1845; (j) J.-K. Sun, Q.-X. Yao, Z.-F. Ju and J. Zhang, *CrystEngComm*, 2010, **12**, 1709; (k) C.-C. Wang, S.-M. Tseng, S.-Y. Lin, F.-C. Liu, S.-C. Dai, G.-H. Lee, W,-J. Shih and H.-S. Sheu, *Cryst. Growth Des.*, 2007, **7**, 1783.

16 (a) P. Cromwell, *Knots and Links*, Cambridge University Press, England, 2004; (b) T. Castle, M. E. Evans and S. T. Hyde, *Progress of Theoretical Physics Supplement No. 191*, 2011, 235.

17 R. S. Forgan, J.-P. Sauvage and J. F. Stoddart, *Chem. Rev.*, 2011, **111**, 5434.

18 (a) T. Castle, M. E. Evans and S.T Hyde, *New J. Chem.,* 2008, **32**, 1484; (b) T. Castle, *Entangled graphs on surfaces in space*, Ph.D. Thesis, Australian National University, Canberra, 2013; http://hdl.handle.net/1885/11978.

19 F. Li, J. K. Clegg, L. F. Lindoy, R. B. Macquart and G. V. Meehan, *Nat. Commun.*, 2011, **2**, 205

20 X.-L. Wang, F.-F. Sui, H.-Y. Lin, C. Xu, G.-C. Liu, J.-W. Zhang and A.-X. Tian, *CrystEngComm*, 2013, **15**, 7274.

21 (a) G.-P. Yang, J.-H. Zhou, Y.-Y. Wang, P. Liu, C.-C. Shi, A.-Y. Fu and Q.-Z. Shi, *CrystEngComm*, 2011, **13**, 33; (b) G.-P. Yang, Y.-Y. Wang, P. Liu, A.-Y. Fu, Y.-N. Zhang, J.-C. Jin, and Q.-Z. Shi, *Cryst. Growth Des.*, 2010, **10**, 1443; (c) T. Liu, J. Lu, L. Shi, Z. Guo and R. Cao, *CrystEngComm*, 2009, **11**, 583.

22 A. L. Spek, *J. Appl. Cryst.,* 2003, **36**, 7.

Table 1. Crystal data for complexes **1** – **3.**

compound	**1**	**2**	**3**
formula	$C_{28}H_{32}N_4O_7Cu$	$C_{28}H_{34}N_4O_8Cu$	$C_{28}H_{34}N_4O_8Cu$
fw	600.12	618.13	618.13
crystal system	Triclinic	Monoclinic	Orthorhombic
space group	$P\bar{1}$	$C2/_C$	*Pmna*
a, Å	8.3326(4)	29.5458(9)	15.8723(8)
b, Å	10.3780(5)	6.3519(2)	12.1103(6)
c, Å	16.5929(9)	18.5588(6)	14.8539(7)
α,°	87.460(3)	90	90
β,°	77.784(3)	125.320(2)	90
γ,°	74.322(3)	90	90
V, $Å^3$	1350.09(12)	2841.88(15)	2855.2(2)
Z	2	4	4
D_{calc}, g/cm^3	1.476	1.445	1.438
F(000)	626	1292	1292
μ(Mo K_α), mm^{-1}	0.863	0.825	0.821
range(2θ) for data collection, deg	$4.76 \le 2\theta \le 52.00$	$3.38 \le 2\theta \le 52.00$	$3.76 \le 2\theta \le 52.00$
independent reflections	5302 [R(int) = 0.1066]	2799 [R(int) = 0.0759]	2924 [R(int) = 0.1033]
data / restraints / parameters	5302 / 0 / 383	2799 / 0 / 201	2924 / 0 / 206
quality–of–fit indicator [c]	1.028	1.009	1.053
final R indices [$I > 2\sigma(I)$] [a,b]	R1 = 0.0652, wR2 = 0.1670	R1 = 0.0624, wR2 = 0.1577	R1 = 0.0750, wR2 = 0.1865
R indices (all data)	R1 = 0.1205, wR2 = 0.2012	R1 = 0.1121, wR2 = 0.1864	R1 = 0.1229, wR2 = 0.2242

[a] $R_1 = \Sigma||F_o| - |F_c|| / \Sigma|F_o|$. [b] $wR_2 = [\Sigma w(F_o^2 - F_c^2)^2 / \Sigma w(F_o^2)^2]^{1/2}$. $w = 1 / [\sigma^2(F_o^2) + (ap)^2 + (bp)]$, $p = [\max(F_o^2 \text{ or } 0) + 2(F_c^2)] / 3$. a = 0.1048, b = 0.4275, **1**; a = 0.1051, b = 0.7142, **2**; a = 0.1126, b = 5.7921, **3**;**.**

[c] quality–of–fit = $[\Sigma w(|F_o^2| - |F_c^2|)^2 / N_{observed} - N_{parameters})]^{1/2}$.

Table 2. Selected Bond Lengths (Å) and Angles (°) for complexes **1 – 3.**

1			
Cu-O(6A)	1.959(4)	Cu-O(3)	1.997(3)
Cu-N(1)	2.001(5)	Cu-N(3)	2.006(5)
Cu-O(5B)	2.173(4)		
O(6A)-Cu-O(3)	150.3(2)	O(6A)-Cu-N(1)	85.3(2)
O(3)-Cu-N(1)	90.9(2)	O(6A)-Cu-N(3)	88.0(2)
O(3)-Cu-N(3)	90.9(2)	N(1)-Cu-N(3)	169.5(2)
O(6A)-Cu-O(5B)	122.9(2)	O(3)-Cu-O(5B)	86.8(1)
N(1)-Cu-O(5B)	97.0(2)	N(3)-Cu-O(5B)	93.4(2)
2			
Cu-O(2A)	1.952(3)	Cu-O(2)	1.952(3)
Cu-N(1)	2.011(4)	Cu-N(1A)	2.011(4)
O(2A)-Cu-O(2)	180.0	O(2A)-Cu-N(1)	90.0(2)
O(2)-Cu-N(1)	90.0(2)	O(2A)-Cu-N(1A)	90.0(2)
O(2)-Cu-N(1A)	90.0(2)	N(1)-Cu-N(1A)	180.0
3			
Cu-O(4A)	1.949(5)	Cu-O(2)	1.970(4)
Cu-N(1B)	2.046(4)	Cu-N(1)	2.046(4)
Cu-O(2C)	2.393(5)		
O(4A)-Cu-O(2)	177.4(2)	O(4A)-Cu-N(1B)	87.4(1)
O(2)-Cu-N(1B)	92.7(1)	O(4A)-Cu-N(1)	87.4(1)
O(2)-Cu-N(1)	92.7(1)	N(1B)-Cu-N(1)	173.7(2)
O(4A)-Cu-O(2C)	95.6(2)	O(2)-Cu-O(2C)	81.8(2)
N(1B)-Cu-O(2C)	92.0(1)	N(1)-Cu-O(2C)	92.0(1)

Symmetry transformations used to generate equivalent atoms: (A) x - 1, y, z. (B) –x + 1, -y + 1, -z + 1 for **1**; (A) -x + 1/2, -y + 1/2, -z + 1 for **2**; (A) x, y - 1, z. (B) –x + 1, y, z. (C) –x + 1, -y + 1, -z + 1 for **3**.

Table 3. Some import parameters of complexes **1** – **3**, $[Cu(\mathbf{L})(1,2\text{-BDC})]_n$ and $\{[Cu(\mathbf{L})(1,3\text{-BDC})(H_2O)]\cdot 3H_2O\}_n$.

Complex	Coordination mode of dicarboxylate ligand	Conformation of **L**	Structure
$\{[Cu(\mathbf{L})(1,2\text{-pda})]\cdot H_2O\}_n$, **1**	μ^3-κ^1,κ^1,κ^1	AAAAA *trans anti-anti* *GGAGG trans anti-anti*	3,5T1
$\{[Cu(\mathbf{L})(1,3\text{-pda})]\cdot 2H_2O\}_n$, **2**	μ^2-κ^1,κ^1	AAAAA *trans anti-anti*	**cds,** 5-fold interpenetration
$\{[Cu(\mathbf{L})(1,4\text{-pda})]\cdot 2H_2O\}_n$, **3**	μ_3-κ^1,κ^1,κ^1	GAAAG *cis syn-syn*	1D self-catenation
$[Cu(\mathbf{L})(1,2\text{-bdc})]_n$	μ^2-κ^2,κ^2	AAAAA *trans syn-syn*[a]	**sql**
$\{[Cu(\mathbf{L})(1,3\text{-bdc})(H_2O)]\cdot 3H_2O\}_n$	μ^2-κ^1,κ^1	GAAAG *trans syn-syn*[a] AAAAA *trans syn-syn*[a]	**cds,** 3-fold interpenetration

[a]Derived from the crystallographic data of $[Cu(\mathbf{L})(1,2\text{-BDC})]_n$ and $\{[Cu(\mathbf{L})(1,3\text{-BDC})(H_2O)]\cdot 3H_2O\}_n$.

Caption

Figure 1. (a) Coordination environment of Cu(II) ion in **1**. Symmetry transformations used to generate equivalent atoms: (A) x - 1, y, z. (B) –x + 1, -y + 1, -z + 1. (b) The Cu(II) ions are interlinked by 1,2-PDA^{2-} ligands to give 1D looped chain. (c) A drawing showing the 3,5-coordinated net with $(4^2.6^5.8^3)(4^2.6)$-3,5T1 topology. (d) A drawing showing the 6-coordinated net with the $(4^{12}.6^3)$-**pcu** topology.

Figure 2. (a) Coordination environment of Cu(II) ion in **2**. Symmetry transformations used to generate equivalent atoms: (A) -x + 1/2, -y + 1/2, -z + 1. (b) The Cu(II) ions are interlinked by 1,3-PDA^{2-} ligands to give 1D linear chains. (c) A drawing showing the 4-connect net with $(6^5.8)$-**cds** topology. (d) A drawing showing the 5-fold interpenetrated network.

Figure 3. (a) Coordination environment of Cu(II) ion in **3**. Symmetry transformations used to generate equivalent atoms: (A) x, y - 1, z. (B) –x + 1, y, z. (C) –x + 1, -y + 1, -z + 1. (b) A drawing showing the 1D chain. (c) A simplified drawing showing the 1D self-catenated structure.

Figure 4. (a) A schematic drawing for **3**. (b) Two equivalent representations of the same arrangement but NOT entangled. (c) A drawing showing the Hopf links. (d) A drawing showing the Solomon links.

Figure 5. Three possible orientations for the pyridyl nitrogen atoms of the **L** ligand. (a) *syn-syn* (b) *syn-anti* (c) *anti-anti*

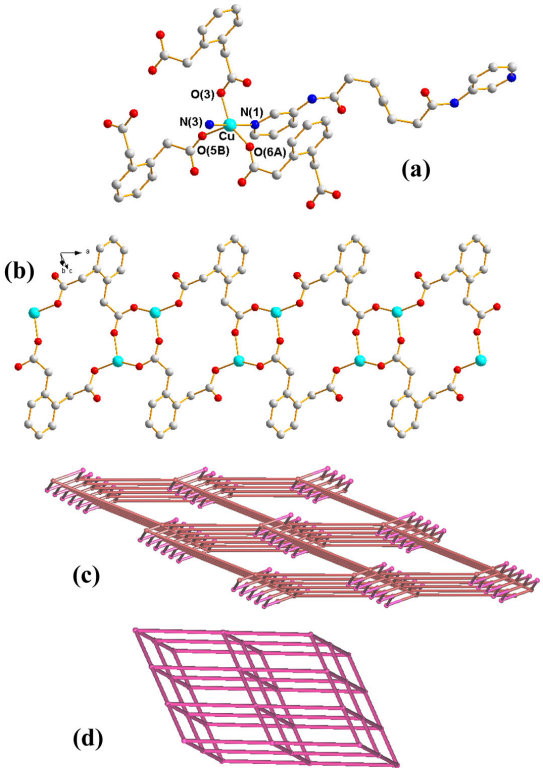

Figure 1

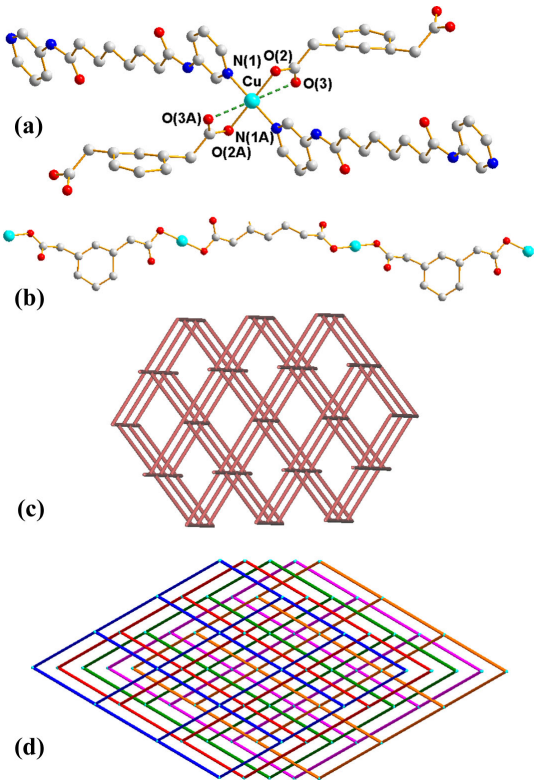

Figure 2 .

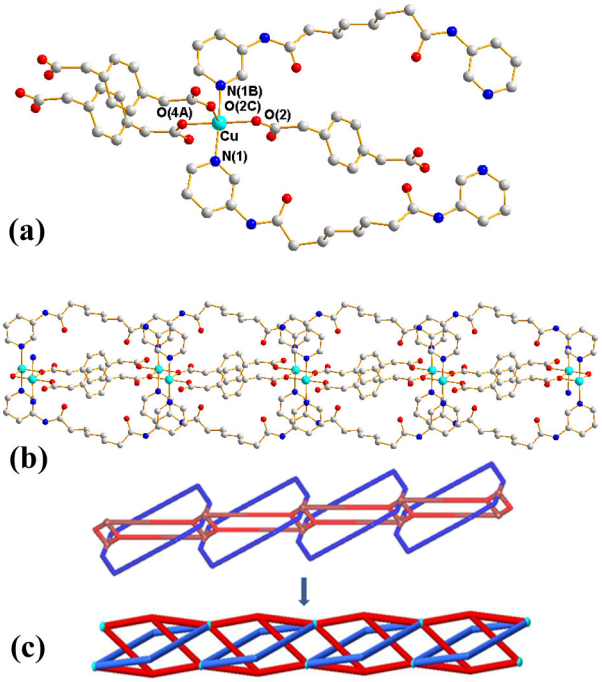

Figure 3

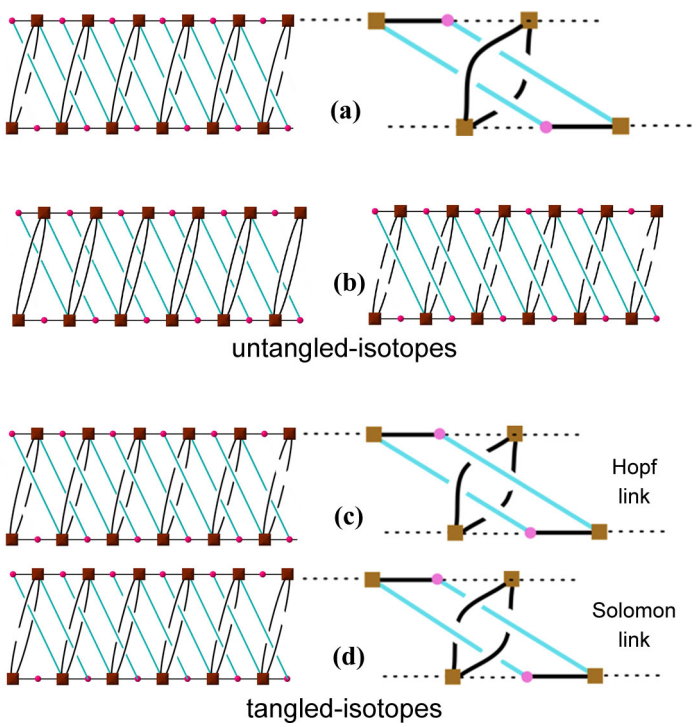

Figure 4

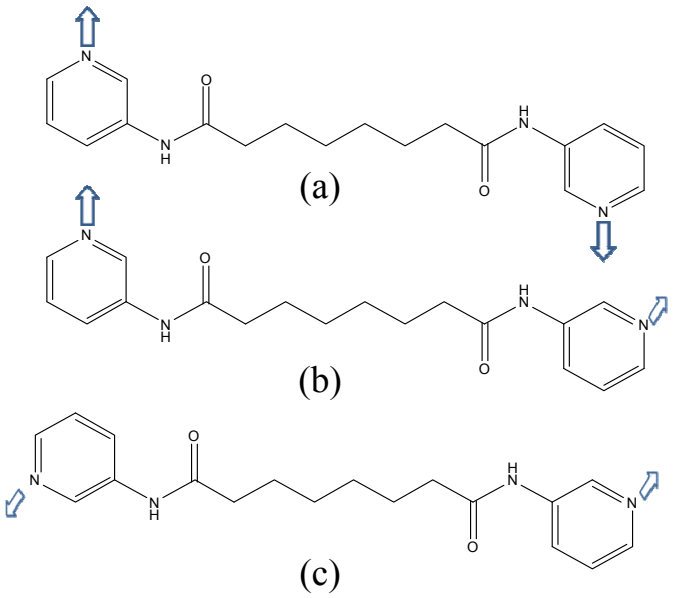

Figure 5